

Electronic Supplementary Material (ESI) for ChemComm.  
This journal is © The Royal Society of Chemistry 2021

### **Supporting Information**

#### **Au-Fe<sub>3</sub>O<sub>4</sub> nanoagent coating with cell membrane for targeted delivery and enhanced chem/photo therapy**

Yingshu Guo,<sup>\*1</sup> Xiuping Cao<sup>2</sup> and Shusheng Zhang<sup>\*2</sup>

<sup>1</sup> Shandong Provincial Key Laboratory of Molecular Engineering, School of Chemistry and Chemical Engineering, Qilu University of Technology (Shandong Academy of Sciences), Jinan 250353, China.

<sup>2</sup> School of Chemistry and Chemical Engineering, Linyi University, Linyi 276005, China.

\*Corresponding email address: yingshug@126.com; shushzhang@126.com

## **EXPERIMENTAL SECTION**

### **Chemicals and reagents**

Benzyl ether and phorbol 12-myristate 13-acetate were obtained from Sigma Aldrich. 1,2,3,4-Tetrahydronaphthalene, Tannic acid, Borane-tert-butylamine complex, 1-Octadecene, 1-Hexadecylamine (HDA), Hydrogen tetrachloroaurate trihydrate ( $\text{HAuCl}_4 \cdot 3\text{H}_2\text{O}$ ) were purchased from Macklin.  $\text{Fe}_2(\text{CO})_9$  and Oleylamine were purchased from Aladin. Oleic acid, MTT cell proliferation and cytotoxicity assay Kit were purchased from Sangon Biotech. 3,3',5,5'-tetramethylbenzidine (TMB) was obtained from Aladdin company. Fetal bovine serum was provided by Thermo Fisher Scientific. MCF-7 human breast cancer cells were purchased from Shanghai Zeye Biotechnology Co., Ltd. All animal experimental procedures and techniques were approved by the Animal Ethics Committee of Linyi University, and methods were carried out in accordance with the approved guidelines and laws.

### **Instrument**

Size and Zeta potential measurement was performed at 25°C on a Zeta-Size Nano instrument (Zen 3600, Malvern Instruments Ltd.). MTT assay was performed on a microplate reader (EP0CH2, China). The ultraviolet (UV)-visible spectra were recorded on a Cary 50 UV-vis-NIR spectrophotometer. Nano-ZS90 zeta potentiometer (Malvern Instrument Ltd., Britain) was used to measure the particle size of the nanomaterials. The cell images were performed on a TCS SP8 II laser confocal microscope (Nikon C2plus, Germany).

## **Cell culture**

All MCF-7 breast cancer cells and A549 cells involved in the experiment were cultured in a constant temperature and humidity box at 37°C, with a humidity of 95% and a CO<sub>2</sub> concentration of 5%. The culture medium used for the cells was DMEM with 10% fetal bovine serum and 1% double antibody (penicillin-streptomycin).

## **Synthesis of HDA·HCl**

The mixed solution contained 1 mL HCl solution and 11 mL ether solution. The mixed solution and 10 mmol HDA were poured in 150 mL of n-hexane, cooled through an ice bath until a white precipitate was formed. After stirring for 2 hours at room temperature, the solution was decanted. The obtained precipitate was washed 3 times with n-hexane, dried and collected for later use.

## **Synthesis of Au NPs**

The mixture was prepared, which was composed of 0.2 g H<sub>2</sub>AuCl<sub>4</sub>·3H<sub>2</sub>O, 1,2,3,4-tetrahydronaphthalene and 10 mL oleylamine. Under the mild flow of nitrogen, the mixture was stirred evenly until the liquid turns orange. The above solution was cooled to 4°C in an ice bath. 1 mL of 1,2,3,4-Tetrahydronaphthalene and 1 mL of oleylamine were added to the test tube, 0.5 mmol of borane-tert-butylamine complex was added into the test tube to fully dissolve. All the liquid in the test tube was poured into the cooled mixed liquid. At this time, the solution appeared dark purple and the reaction lasted for 2h. After the reaction of the solution was complete, 50 mL of acetone was added, then the liquid was centrifuged (10000 r/min, 8min) to collect the nanoparticles. 20 mL n-hexane, 50 mL ethanol were added, and the liquid was centrifuged again (9000

r/min, 8min) to wash the product. The final product obtained was stored in an environment of 4°C with n-hexane.

### **Synthesis of Au–Fe NPs**

Under argon flow, 1 mmol of HDA·HCl solution was mixed with 12 mL of 1-octadecene and 1 mL of oleylamine. The mixed solution was fully stirred and heated to 120°C, then 24 mg Au NP was added to the mixed solution and degassed for 30 min. The solution was further heated to 180°C, the liquid is cooled slightly, 1 mmol of Fe<sub>2</sub>(CO)<sub>9</sub> was added, and the reaction continued for 30 min and then cooled to room temperature. 45 mL isopropanol was added and the product was collected by centrifugation (8500 r/min, 8min). Then the product was washed. 20 mL of n-hexane, 50 mL of ethanol were added and then centrifuge (8500 r/min, 8min). The obtained product was stored in n-hexane and placed in an environment of 4°C.

### **Synthesis of Au–Fe<sub>3</sub>O<sub>4</sub> NPs**

The product Au–Fe NPs obtained in the supporting information step was mixed with 20 mL of 1-octadecene and 1 mL of oleylamine, and heated to 160°C. Under the flow of N<sub>2</sub>, and the reaction continued for 15 min. When the liquid was cooled to room temperature, it was collected and purified according to the above method.

### **Synthesis of micropore Au–Fe<sub>3</sub>O<sub>4</sub> NPs (AF)**

Under the gentle flow of Ar, 50 mg of Au-Fe<sub>3</sub>O<sub>4</sub> nanoparticles, 0.08 mL of oleylamine, 0.08 mL of oleic acid and 10 mL of benzyl ether were mixed. Then they were transferred to a three-necked flask and degassed at room temperature

for 30 min. The mixture was then magnetically stirred and heated to 240°C at a rate of 5°C per minute, kept at this temperature for 30 min, and then cooled to room temperature. The product was collected and purified according to the previous method.

#### **Acquisition of MCF-7 cell membrane**

When MCF-7 cells were grown in a cell culture dish (10 cm diameter) until they were fully confluent, 1 mL of trypsin was added at a humidity of 95%, a CO<sub>2</sub> concentration of 5%, and incubated in a cell incubator at 37°C for 1 minute at a constant temperature. Then 5 mL of DMEM supplemented with double antibodies and fetal calf serum was added to prevent digestion, and the cells were transferred to a 15 mL centrifuge tube for centrifugation. After pulverizing the obtained cells with an ultrasonic cell pulverizer, they were centrifuged at 2500 rpm at 4°C for 10 min. The precipitate was removed, the supernatant was centrifuged at 15000 rpm for 20 min, and the final precipitate was collected and used for subsequent experiments.

#### **The fabrication of the AFTP@CM**

100 μL Au-Fe<sub>3</sub>O<sub>4</sub> with 100 μL tannic acid (4.5 mg/mL) and 20 μL PMA (0.1 mg/mL) were incubated for 6 hours to obtain AFTP. Then the prepared MCF-7 cell membrane was mixed with AFTP, and the resulting mixture was sonicated for 40 min to obtain AFTP@CM. AFTP@CM was put into a test tube and placed on the magnetic stand. One minute later, we aspirated the liquid. Next, we added PBS into the test tube and sonicated for one minute, placed it on the magnetic

stand again. This operation was repeated three times to remove excess cell membranes. The fabrication processes of AFT@CM, AFP@CM, AF@CM were followed the similar methods.

### **Cytotoxicity experiments**

MCF-7 cells and A549 cells were incubated with AFTP@CM, AFT@CM, and AFP@CM in a cell culture incubator for 3, 6, 9, 12, and 24 hours, respectively. The supernatant in each well was aspirated carefully. Then, 10  $\mu$ L MTT and 90  $\mu$ L of fresh medium were added into each well, and keep at 37°C for 4 hours. 4 hours later, the supernatant was aspirated, 110  $\mu$ L of Formazan dissolving solution was added, it was shaken on a shaker at low speed for 10 minutes, then detected at 490 nm by a microplate reader.

### **Photothermal efficiency test of materials**

AFTP@CM and PBS were irradiated by 808 nm laser with the power of 3.52 W  $\text{cm}^{-2}$ , stay 5 min. Within 5 min, we get temperature images of samples at different times by the infrared thermal imager, and the temperature curve was obtained according to the temperature change data.

### **Cell internalization experiment**

The prepared cell membrane was stained with DiI fluorescent dye, and AFTP@CM was prepared with the stained cell membrane. MCF-7 cells (1 mL,  $1 \times 10^5$  cells) and A549 cells (1 mL,  $1 \times 10^5$  cells) were stained with DAPI fluorescent dye in their nuclei, and then incubated with AFTP@CM for 30 min

and 60 min, respectively. The TCS SP8 II laser confocal microscope was used to observe and take pictures for cell tracking.

### **Cytotoxicity test of AFTP@CM by calcein AM/PI**

To distinguish between living and dead cells,  $10^4$  MCF-7 cells were poured in each small petri dish for 12 hours later. Then, AFT@CM, AFP@CM, and AFTP@CM was added into the small petri dish, respectively. After 24 hours, the supernatant was aspirated, the cells were washed with PBS, and stained with propidium iodide (PI, 4  $\mu$ M) and calcein AM (2  $\mu$ M) for 2 hours. Finally, we used the TCS SP8 II laser confocal microscope to observe and take pictures. Similarly, an A549 control group was set up for observation and comparison.

### **Cellular uptakes**

$1 \times 10^5$  MCF-7 cells and A549 cells were cultured in small dishes for 12 hours. The MCF-7 cells were incubated with AFTP@CM (2.0 mg.ml<sup>-1</sup>) for 0.5 hours, 1 hour and 3 hours, respectively. The same for A549 cells. The cells were obtained by trypsin digestion, and then rinse with PBS 3-5 times. The obtained cells are tested for element content through ICP-OES.

### **Intracellular AFTP@CM Fenton reaction effect**

$1 \times 10^5$  MCF-7 cells was cultured in small dishes for 12 hours. Then MCF-7 cells incubate with DCFH-DA kit. 20 min later, DCFH-DA in the small dish was rinsed off by PBS. Next, the cells were incubated with AFTP@CM and PBS, respectively. 30 min later, AFTP@CM for 30 min. The cells were washed 3-5

times with PBS, and then the cells were washed 3-5 times with PBS and observed by a confocal microscope.

### **Construction of MCF-7 tumor-bearing mouse model**

All MCF-7 tumor-bearing mice are NOD SCID mice of 4-5 weeks old. Each mouse was injected with MCF-7 cells ( $5 \times 10^6$  cells/mouse) subcutaneously. Body weight and tumor volume were measured every day. When the tumor grew to 100-150 mm<sup>3</sup>, they were divided into 4 groups (PBS group, PBS+Laser group, AFTP@CM group, AFTP@CM+Laser group) according to our experimental plan, and different treatment plans were implemented according to the group.

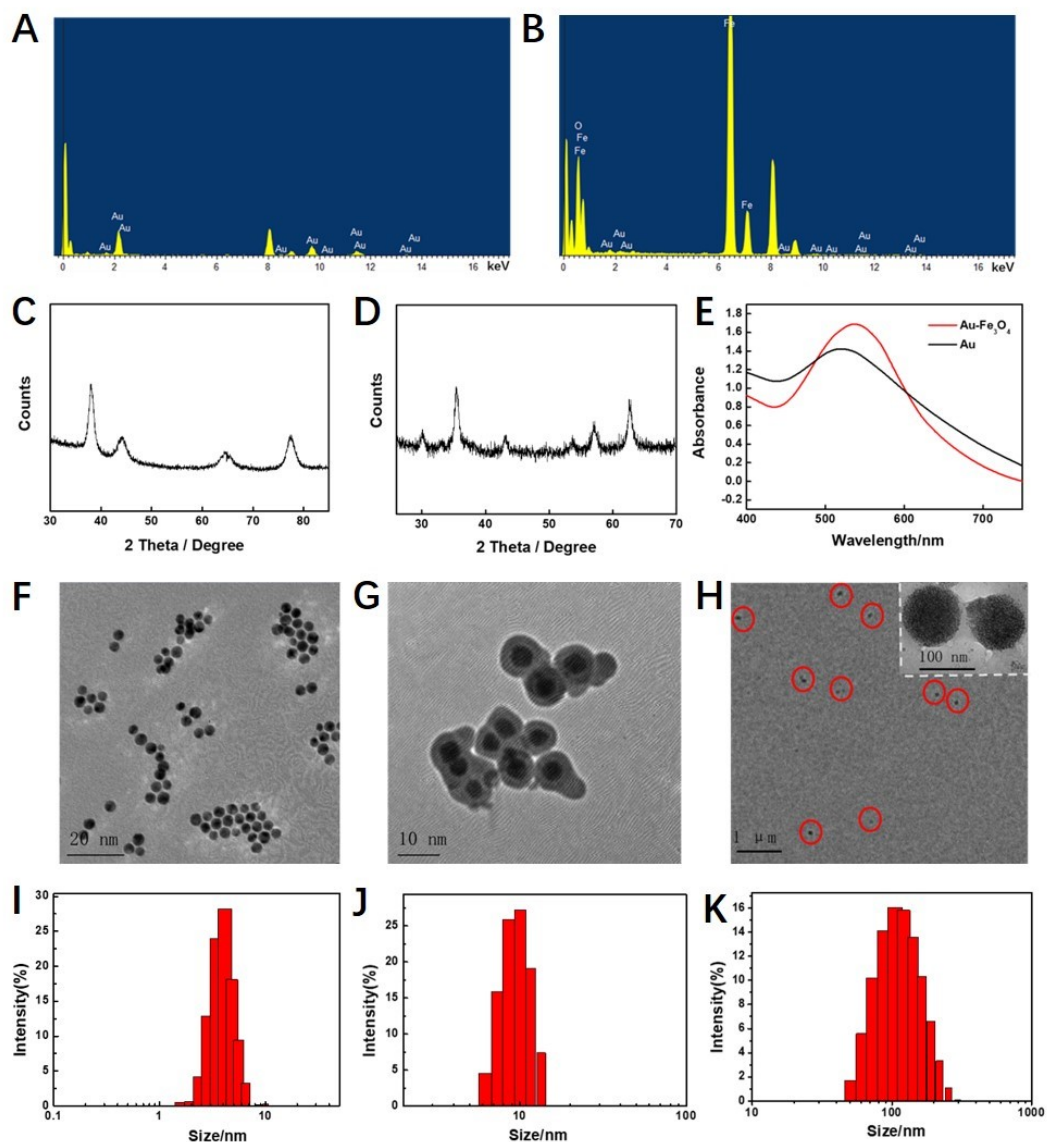


**Fig. S1** (A) (B) EDS analysis of Au nanoparticles and AF. (C) (D) XRD analysis of Au nanoparticles and AF. (E) UV-vis spectra of Au nanoparticles and AF. (F) (G) (H) TEM images of Au nanoparticles, AF and AFTP@CM. (I) (J) (K) Particle size of the Au, nanoparticles AF and AFTP@CM.

Based on the synthesis of Au nanoparticles, AF was synthesized and incubated with TA and PMA to obtain AFTP. Then, MCF-7 CM was coated on AFTP by extrusion, and the final product was obtained AFTP@CM. In Fig. S1AB, the EDS analysis data proves the successful preparation of Au nanoparticles and AF. In order to explore what

kind of oxide ( $\text{Fe}_2\text{O}_3$ ,  $\text{Fe}_3\text{O}_4$  or others) is in AF, we tested Au nanoparticles and AF through X-ray diffraction (XRD) patterns. The peaks of Au nanoparticles and oxide are shown in Fig. S1. The characteristic peaks of Au nanoparticles and oxide are consistent with those reported in the literature.<sup>1-2</sup> Therefore, the oxidation state of iron in AF is  $\text{Fe}_3\text{O}_4$ . In addition, in the UV-vis analysis, Au nanoparticles showed a maximum absorption at 520 nm, while the maximum absorption of Au- $\text{Fe}_3\text{O}_4$  was around 550 nm (Fig. S1E).<sup>1</sup> Through the transmission electron microscope images, we found that the average size of Au nanoparticles is about 4 nm, while that of AF nanoparticles is about 10 nm, AFTP@CM The average particle size is about 100 nm (Fig. S1FGH). A series of results showed that AF nanoagent was successfully prepared. The size of the nanoparticles was further tested by dynamic light scattering, and the results were basically consistent with the transmission electron microscope images (Fig. S1IJK).

In Fig. S2A. We can see that the pore size of most micropores is about 1.2 nm, which makes the loading of TA and PMA more convenient and effective. And through the observation of different sizes of nanoparticles, we preliminarily believe that CMs successfully encapsulates multiple AFTPs. In order to verify this idea, we analyzed the zeta potential of AFTP, CM and AFTP@CM, and the results revealed that CM had strong electronegativity, and the electronegativity of AFTP@CM was stronger than that of pure AFTP (Fig. S2B). Besides, AFTP@CM was investigated by SDS-PAGE (Fig. S2C). The results show that there is no obvious phenomenon in AFTP, while the phenomenon of AFTP@CM is roughly the same as that of CM. This phenomenon confirms our idea that CM has been successfully coated on AFTP.

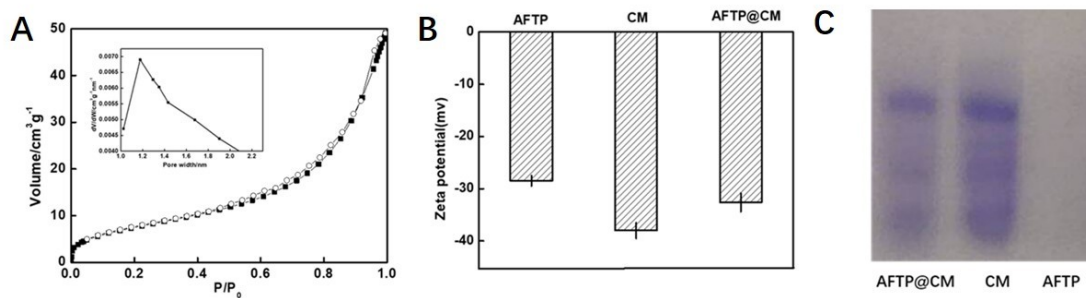


**Fig. S2** (A) Nitrogen adsorption–desorption isotherm of AF. Inset: pore size distribution. (B) Particle zeta potential of the AFTP, CM and AFTP@CM. (C) SDS-PAGE images of AFTP@CM, CM and AFTP.

In order to test the in vitro photothermal effect of AFTP@CM, we verified it. Under irradiation with an 808 nm NIR laser with the power density of  $3.5 \text{ W cm}^{-2}$ , we observed and recorded the temperature rise of AFTP@CM and PBS. It was observed that the temperature of AF solution increased rapidly to about  $67^\circ\text{C}$  under 808 nm laser irradiation, while the temperature of PBS did not increase significantly (Fig. S3A). In the temperature time curve, we more accurately verify the excellent PTT effect of AFTP@CM (Fig. S3B), which is our nanoagent AFTP@CM. The application in PTT provides guarantee.

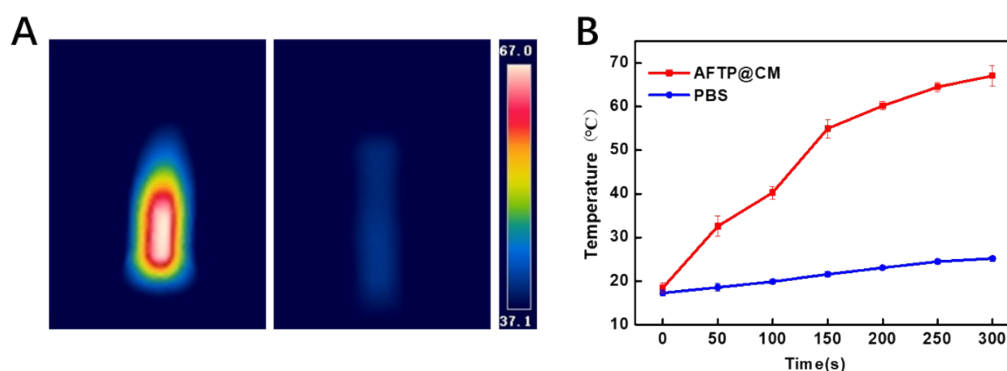


**Fig. S3** (A) Photothermal images of AF and PBS. (B) The temperature changes of AFTP@CM and PBS under 808 nm laser irradiation.

In our experiments, AF and AFT were put into two test tubes and H<sub>2</sub>O<sub>2</sub> was added. After a period of reaction, TMB was added to two test tubes respectively. TA can promote the conversion of Fe<sup>3+</sup> to Fe<sup>2+</sup>, and the presence of Fe<sup>2+</sup> is conducive to the production of a large number of hydroxyl (•OH).<sup>3-4</sup> TMB can be oxidized to a colored oxidation product (oxTMB) under the action of •OH.<sup>5-7</sup> Based on this principle, after 10 minutes, we observe the two sets of samples. We found that the tube without TA was light blue, and the tube with TA was color burn. Because the solution of TMB reacted with •OH has UV absorption at 650 nm, we detected the liquid in the two tubes on the UV spectrophotometer, and found that the UV absorption of AFT group was significantly higher than that of AF group at 650 nm (Fig. S4A). This phenomenon further supports the role of TA. TA as a reducing agent can effectively accelerate the process of Fe<sup>3+</sup> to Fe<sup>2+</sup> conversion, and improve the efficiency of the CDT reaction.

In the separation process of AFTP@CM, we found that it has a remarkable magnetic separation effect, as shown in Fig. S4B, it can be quickly separated under the action of magnetic force. This property provides great convenience for our later experimental operation, and has potential in magnetic targeting and imaging.

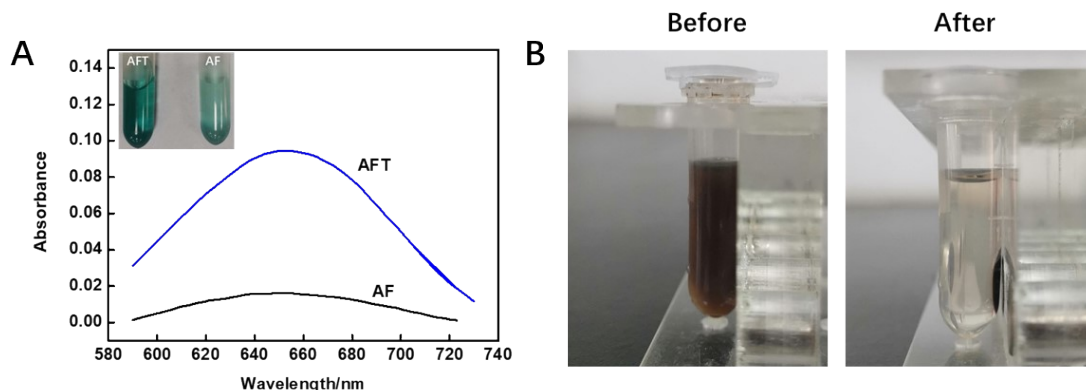


**Fig. S4** (A) Pictures and UV-vis spectra of AFT and AF after adding TMB. (B) Magnetic separation image of AFTP@CM.

After AFTP@CM enters the cell, it will cause a strong Fenton reaction and generate a large amount of ROS. In order to verify the effect of AFTP on the Fenton reaction to produce ROS, we used the DCFH-DA kit to detect ROS in cells. DCFH-DA was incubated with MCF-7 cells for 20 minutes respectively. Then MCF-7 cells rinsed with PBS 3-5 times, 10  $\mu$ L AFTP@CM and PBS was added in two small dishes respectively. After 30 minutes, the cells were rinsed with PBS 3-5 times, and placed under a confocal microscope for observation. As shown in Fig. S5, the cells treated with PBS have extremely weak fluorescence, while the cells treated with AFTP@CM have strong fluorescence. This phenomenon fully demonstrates that AFTP@CM entered the cell smoothly, and carried out a relatively strong Fenton reaction in the cell, which produced a large amount of ROS.

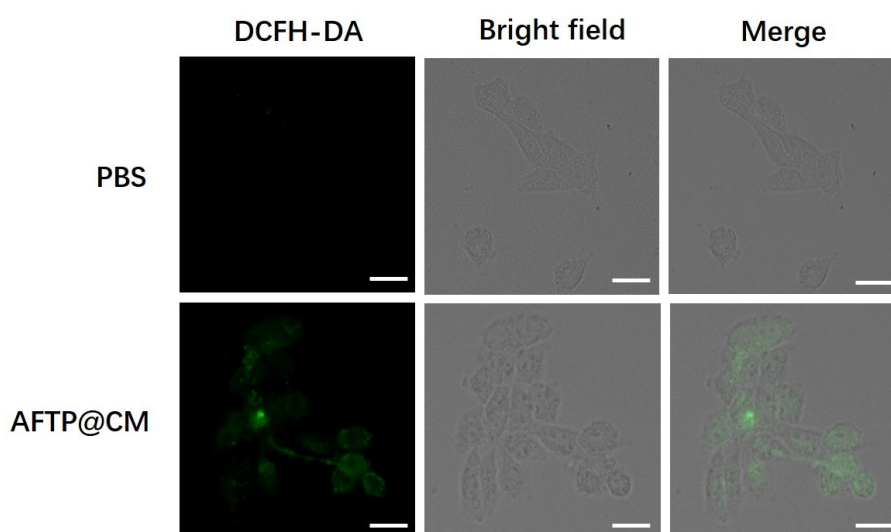


**Fig. S5** Confocal laser scanning microscopy (CLSM) images of MCF-7 cells ,which treated with PBS and AFTP@CM respectively. Scale bar: 20  $\mu$ m.

In order to verify the biodistribution of AFTP@CM in mice, we set up one group of mice (AFTP@CM+Laser). The hair on the tumor site of the mouse was cleaned up for observation. After 24 hours of drug injection, mice were irradiated whole body with an 808 nm NIR laser with a power density of  $3.5 \text{ W cm}^{-2}$ . The temperature of the tumor site increased rapidly, and the temperature difference with other parts of the body was large (Fig. S6). This indicates that the photothermal effect is stronger at the tumor site in mice, while the other sites are weaker. Therefore, AFTP@CM is mainly distributed in tumors in mice.

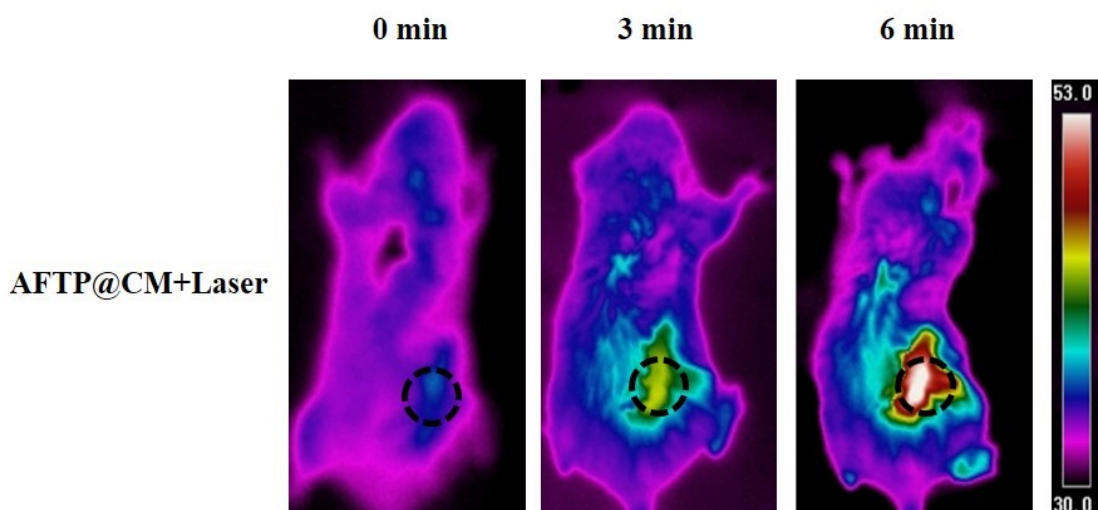


**Fig. S6** Pictures of the whole body temperature changes in tumor-bearing mice (AFTP@CM+Laser).

## References

- 1 G.-M. Jiang, Y.-X. Huang, S. Zhang, H.-Y. Zhu, Z.-B. Wu and S.-H. Sun, *Nanoscale*, 2016, **8**, 17947.
- 2 Q. Gao, A.-W. Zhao, H.-Y. Guo, X.-C. Chen, Z.-B. Gan, W.-Y. Tao, M.-F. Zhang, R. Wu and Z.-X. Li, *Dalton Trans.*, 2014, **43**, 7998.
- 3 Y.-X. Guo, H.-R. Jia, X.-D. Zhang, X.-P. Zhang, Q. Sun, S.-Z. Wang, J. Zhao and F.-G. Wu, *Small*, 2020, **16**, 2000897.
- 4 H.-M. Zhu, G.-D. Cao, C. Qiang, Y.-K. Fu, Y.-L. Wu, X. Li and G.-R. Han, *Biomater. Sci.*, 2020, **8**, 3844-3855.
- 5 S. Ahmed, J. Cirone and A. Chen, *ACS Appl. Nano Mater.*, 2019, **2**, 2076–2085.
- 6 T. Zhang, S. Zhang, J. Liu, J. Li and X. Lu, *Anal. Chem.*, 2020, **92**, 3426–3433.
- 7 L. Gao, J. Zhuang, L. Nie, J. Zhang, Y. Zhang, N. Gu, T. Wang, J. Feng, D. Yang, S. Perrett and X. Yan, *Nat. Nanotechnol.*, 2007, **2**, 577.